Coordinate Control of Energy Saving Programmable Valves

Song Liu and Bin Yao, *Member, IEEE*

***Abstract*—As applications of electro-hydraulic systems become increasingly widespread, the demand for *low cost*, *high-level control performance* and *significant energy saving* schemes gets stronger and stronger. The recently developed energy-saving programmable valves, a unique configuration of five independently controlled poppet type cartridge valves, provide hardware possibility to meet the demand. Preliminary research work has shown that the program valves' increased flexibility and controllability lead to significant energy-saving, due to the reduced working pressures of the hydraulic actuators and the full use of free regeneration cross-port flows. However, the increased hardware flexibility also results in increased complexity in controlling the system: for each system, instead of one control input to be synthesized to meet the sole objective of control performance, five control inputs have to be simultaneously determined for all five poppet valves to achieve the dual objectives of both high precision control performance and significant energy saving. This paper proposes a two-level coordinated control scheme: the task-level configures the valve usage for maximal energy saving and the valve-level utilizes adaptive robust control (ARC) technique to guarantee the closed-loop system stability and performance under various model uncertainties and disturbances. Comparative experimental results were obtained to show the high precision control performance and significant energy saving achieved with the proposed low-cost programmable valves.**

***Index Terms*—Adaptive robust control, coordinated control, electro-hydraulics, energy saving, valves.**

I. Introduction

THE ADVENT OF electro-hydraulic valves and the incorporation of complex digital control have significantly improved the performance of hydraulic systems. A new problem arises as the applications of electro-hydraulic systems become increasingly widespread: is it possible to reduce the energy usage while keeping the desired control performance? Such a problem has become increasingly important due to the potential energy crisis that the world is going to face. The recently proposed energy-saving programmable valves, as shown in Fig. 1, provide hardware possibility to meet the demand.

Manuscript received February 5, 2006; revised October 24, 2006. Manuscript received in final form March 25, 2007. Recommended by Associate Editor C. Y. Su. This paper was presented in part at the ASME IMECE'03, Washington, D.C. This work was supported in part by the National Science Foundation under Grant CMS-0600516 and by the National Natural Science Foundation of China (NSFC) under the Joint Research Fund Grant 50528505 for Overseas Chinese Young Scholars.

S. Liu is with Hurco Companies, Inc., Indianapolis, IN 46268 USA (e-mail: mail.liusong@gmail.com)

B. Yao is with the School of Mechanical Engineering, Purdue University, West Lafayette, IN 47907-2040 USA and also with The State Key Laboratory of Fluid Power Transmission and Control, Zhejiang University, Hangzhou 310027, China (e-mail: byao@purdue.edu).

Digital Object Identifier 10.1109/TCST.2007.903073

The use of programmable valves provides multiple inputs to control the two cylinder states, the pressures P_1 and P_2 of the two chambers of the cylinder. The result is that both cylinder states become completely controllable and the true cross port regeneration flow can be accurately controlled. However, to control such a multi-input nonlinear system to meet the dual objectives of high control performance and significant energy saving is far from trivial. The difficulties to control the programmable valves not only come from the highly nonlinear hydraulic dynamics, large parameter variations [23], significant uncertain nonlinearities such as external disturbances, flow leakages, and seal frictions [17], [25], but also from the lack of accurate mathematical model of cartridge valves and the coordinated control of the five cartridge valves. To simplify the controller design process, our preliminary work assumed a constant offside pressure [16]. This assumption may not be realistic in certain circumstances where the offside pressure may vary from the assumed constant pressure significantly, especially right after the change of working modes. As a result, though the controller design is simplified, larger tracking errors may exhibit during transients.

This paper focuses on the coordinate control of programmable valves and proposes a two-level control scheme to address the previous challenges. Specifically, the task level controller determines the configurations of programmable valves that would enable significant energy saving while without losing hydraulic circuit controllability for accurate motion tracking, which is sometimes referred to as the working mode selection in hydraulic industry. With the selected working mode, the valve level controller regulates the pressures in both chambers of the cylinder independently to meet the dual objectives of precise motion tracking and energy saving. Experimentally obtained valve flow mappings are used to overcome the lack of mathematical models of cartridge valves. The nonlinear physical model-based adaptive robust control (ARC) technique [27]–[29] is employed to explicitly deal with parametric uncertainties and uncertain nonlinearities for a better control performance.

II. Development of Energy-Saving Programmable Valves

Hydraulic energy used for a task can be defined as

$$E = \int_{t_0}^{t_1} P_s(\tau) Q_s(\tau) d\tau \tag{1}$$

where E represents the hydraulic energy used for a certain task from t_0 to t_1, P_s, and Q_s are the hydraulic supply pressure and flow rate of the pump, respectively. For a specific task, i.e., t_0

and t_1 are fixed, reducing the energy usage is equivalent to reducing the power, i.e., the integrand $P_s(t)Q_s(t)$. Therefore, the word energy is abused for both energy and power thoughout this paper. It is obvious that there may be the following two ways to reduce the energy usage:

1) *reduce the supply pressure* $P_s(t)$;
2) *reduce the pump flow rate* $Q_s(t)$.

Neglecting the fluid compressibility, the pump flow rate depends only on the task unless regeneration flows are used. To reduce the supply pressure, pressures at the two cylinder chambers are desired to be as low as possible while certain pressure difference has to be kept to perform the required motion. Therefore, independent control of two chamber pressures and the use of regeneration flows are the two key elements for energy saving.

Traditionally, a four-way proportional directional control (PDC) valve or servo valve is used to control each hydraulic cylinder as assumed in almost all existing publications [5], [7], [17], [18], [20], [25]. With such a configuration only one of the two cylinder states is completely controllable and there is a 1-D internal dynamics. Although the internal dynamics is shown to be stable [4], it cannot be modified by any motion trajectory tracking control strategy. The control input is uniquely determined once the desired motion is specified, which makes the regulation of individual cylinder chamber pressures impossible. The result is that while high performance tracking may be attainable, simultaneous high levels of energy saving cannot. The uncontrollable state is due to the fact that the meter-in and meter-out orifices are mechanically linked together in a four-way valve. If this link were to be eliminated, the hardware flexibility could be drastically increased, making the way for significant improvements in hydraulic efficiency [12].

The technique of eliminating the mechanical linkage between the meter-in and meter-out orifices is well known and has been used in heavy hydraulic industry for years. For example, Aardema [1] makes use of two directional control valves. One valve controls the head end chamber flows and the other controls the rod end chamber flows. One drawback to this approach is that two directional control valves are needed at an increased cost. The other drawback is that the control of the meter-in and meter-out flows are not completely independent.

A more widely used variation is the use of four independent valves of either one-way unidirectional type or poppet type, allowing truly independent meter-in and meter-out flow controls. This is used in a number of studies throughout the mobile hydraulics industry [2], [3], [14]. The use of this "Smart Valve" [3] or "Independent Metering Valve" [2] provides the hardware capability of independent control of each meter-in and meter-out ports, resulting in the ability to completely control both cylinder states. This hardware flexibility can be used to meet the dual objectives of precise motion tracking control and high energy efficiency to a certain degree when properly utilized.

Besides eliminating the meter-in and meter-out flow coupling, energy saving can also be obtained by taking advantage of regeneration flow [8]. Regeneration flow is the fluid pumped from one chamber to the other chamber by the energy of the external load. Regeneration is a highly efficient process in which little or zero pump energy is needed. Ideally, regeneration should be used whenever the external force is in the same direction as the desired motion to attain maximum energy efficiency. The four-valve metering unit enables the use of regeneration flow in some extreme conditions [2] but not to the fullest extent possible; the pressures at the cylinder chambers must be higher than the pump supply pressure in order to use regeneration flows. Furthermore, precise control of the regeneration flows is not attainable with this set of hardware because a direct cross port flow path does not exist. As such, it is impossible to achieve simultaneous precision motion control performance when regeneration flows are used. Partly because of these difficulties, no results on the simultaneous precise motion tracking and significant energy saving are published yet.

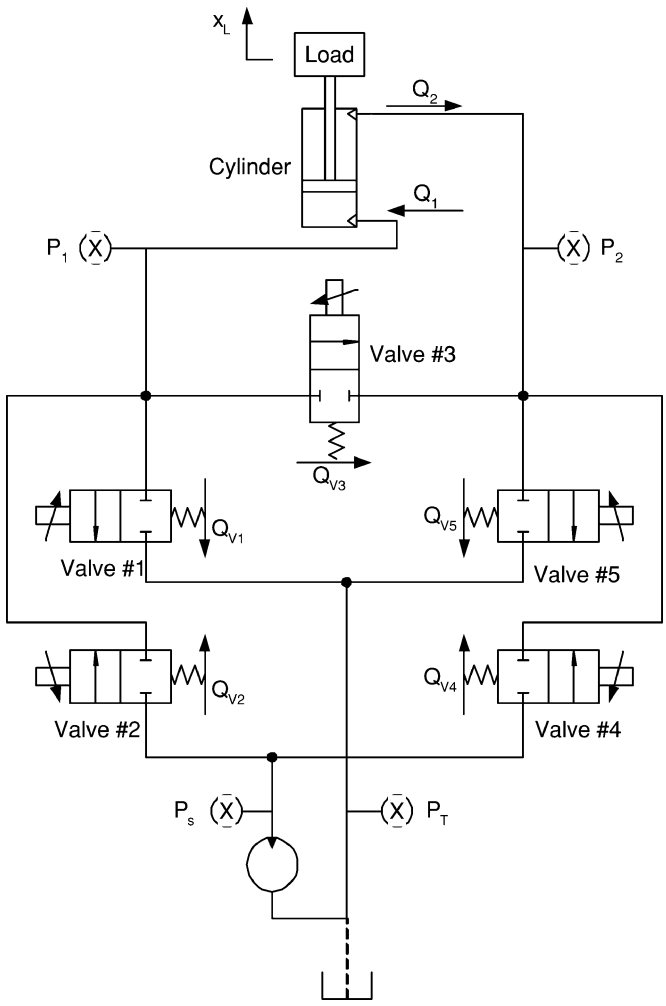

Fig. 1. Programmable valves configuration.

The five-valve energy saving programmable valves shown in Fig. 1 were developed by Yao and his students during the past several years [16], [26] to take full advantage of the four-valve metering mechanism in decoupling the meter-in and meter-out flow regulations [2] and the addition of a fifth valve to enable the precise control of direct cross port flow. The result is a set of programmable valves capable of independently controlling each cylinder state as well as providing fully controlled regeneration flows for maximum energy saving and simultaneous

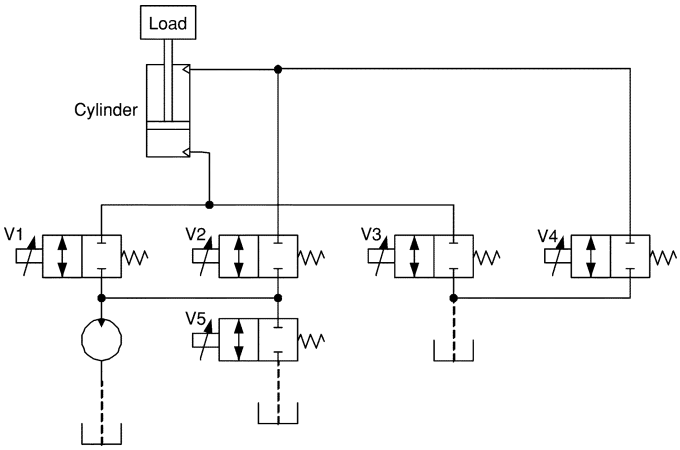

Fig. 2. Five-valve meter-in and meter-out.

precise motion tracking. To significantly reduce the manufacturing cost, the proposed programmable valves use proportional poppet-type cartridge valves, which are known as economical alternatives to large proportional valves [21], though their flow mappings are more complex and hard to obtain accurately.

It should be noted that the proposed five-valve configuration is fundamentally different from other five-valve programmable valves in the literature. Specifically, the work done by Hu and Zhang in [10] and [11] also used a set of five individually controlled E/H valves for flow and pressure controls. The schematic diagram of their programmable valves is shown in Fig. 2. It is obvious that the valves 1–4 provide the same functionality as the four-valve metering unit [2] and the fifth valve (V5) connects the pump and the tank directly and provides a dual-function of line release and an equilibrium port of P-to-T in a direction control valve. Thus, precise control of cross-port flow is not available with this set of hardware configuration as opposed to the proposed ones shown in Fig. 1.

III. Dynamic Models and Problem Formulation

To illustrate the benefits of the proposed programmable valves, they are used to control the boom motion of a three degree-of-freedom (DOF) electro-hydraulic robot arm which was built to mimic the industrial backhoe or excavator arms studied in [25]. With the coordinate systems, joint angles and physical parameters of the system defined in Fig. 3, the boom motion dynamics with the other two joints fixed can be described by [5], [16]

$$\left(J_c + m_L \ell_e{}^2\right)\ddot{q}_2 = \frac{\partial x_L}{\partial q_2}(P_1 A_1 - P_2 A_2) - G_c(q_2) - m_L g \ell_g(q_2) - D_f \cdot \dot{q}_2 + T(t, q_2, \dot{q}_2) \quad (2)$$

where q_2 represents the boom joint angle, x_L represents the boom cylinder displacement, J_c is the moment of inertia of the boom without payload, m_L represents the mass of the unknown payload, G_c is the gravitational load of the boom without payload, P_1 and P_2 are the head and rod end pressures of the cylinder, respectively, A_1 and A_2 are the head and rod end ram areas of the cylinder, respectively, D_f is the damping and viscous friction coefficient and T represents the lumped disturbance torque including external disturbances and terms like the unmodelled friction torque. The specific forms of $J_c, G_c(q_2), l_g(q_2)$, and l_e^2 can be found in [5]. The moment of inertia and the gravity force both depend on the unknown payload m_L. For notational simplicity, they are split into two parts in (2). The first parts, J_c and $G_c(q_2)$, are their values under no payload situation, and the second parts, the terms $m_L g l_g(q_2)$ and $m_L l_e^2$, are the additional values due to the unknown payload m_L. The second parts will be estimated online later via real-time parameter adaptation.

Neglecting cylinder flow leakages, the hydraulic cylinder equations can be written as [17]

$$\begin{aligned} \frac{V_1(x_L)}{\beta_e}\dot{P}_1 &= -A_1 \dot{x_L} + Q_1 = -A_1 \frac{\partial x_L}{\partial q_2}\dot{q}_2 + Q_1 \\ \frac{V_2(x_L)}{\beta_e}\dot{P}_2 &= +A_2 \dot{x_L} - Q_2 = +A_2 \frac{\partial x_L}{\partial q_2}\dot{q}_2 - Q_2 \end{aligned} \quad (3)$$

where $V_1(x_L) = V_{h1} + A_1 x_L$ and $V_2(x_L) = V_{h2} - A_2 x_L$ are the total cylinder volumes of the head and rod ends including connecting hose volumes, respectively, V_{h1} and V_{h2} are the initial control volumes when $x_L = 0, \beta_e$ is the effective bulk modulus. Q_1 and Q_2 are the supply and return flows, respectively.

When the programmable valves in Fig. 1 are used to control the boom motion, Q_1 and Q_2 are given by

$$\begin{aligned} Q_1 &= +Q_{v2} - Q_{v1} - Q_{v3} \\ Q_2 &= -Q_{v3} - Q_{v4} + Q_{v5} \end{aligned} \quad (4)$$

where $Q_{vi},\ i = 1, 2, \ldots 5$, is the orifice flow through the ith cartridge valve and can be described by

$$Q_{vi} = f_{xi}(\Delta P_{vi}, x_{vi}), \quad i = 1, 2, \ldots, 5 \quad (5)$$

in which f_{xi} is the nonlinear orifice flow mapping as a function of the pressure drop ΔP_{vi} and the orifice opening x_{vi} of the ith cartridge valve. According to the valve manufacturer's data sheet, the valve dynamics between x_{vi} and the command voltage u_{vi} to the ith valve can be modeled by a second-order transfer function with a natural frequency of $\omega_v = 353.6$ rad/s and damping ratio of $\zeta_v = 1.03$, which is of sufficiently high bandwidth to be neglected in the controller design stage as done in this paper. The dual objectives of this study can then be stated as follows.

- *Performance.* Given the desired motion trajectory $q_d(t)$, the primary objective is to synthesize control signals for the five cartridge valves (i.e., $u_{vi}, i = 1, \ldots, 5$) such that the output $q_2(t)$ tracks $q_d(t)$ as closely as possible in spite of various model uncertainties.
- *Energy Usage.* The secondary objective is to minimize the overall energy usage.

The following notations will be used throughout this paper. Let $\theta = [\theta_1, \theta_2, \ldots, \theta_n]$ denote a suitably selected unknown parameter vector in the system dynamic equation and $\hat{\theta}$ denote the estimate of θ and $\tilde{\theta}$ the estimation error (i.e., $\tilde{\theta} = \hat{\theta} - \theta$). Let $\theta_{\max} = [\theta_{1\max}, \ldots, \theta_{n\max}]$ and $\theta_{\min} = [\theta_{1\min}, \ldots, \theta_{n\min}]$ be the upper and lower bound of the unknown parameter vector θ, respectively, i.e., $\theta_{\min} \le \theta \le \theta_{\max}$, in which the operation $<$ for two vectors is performed in terms of the corresponding

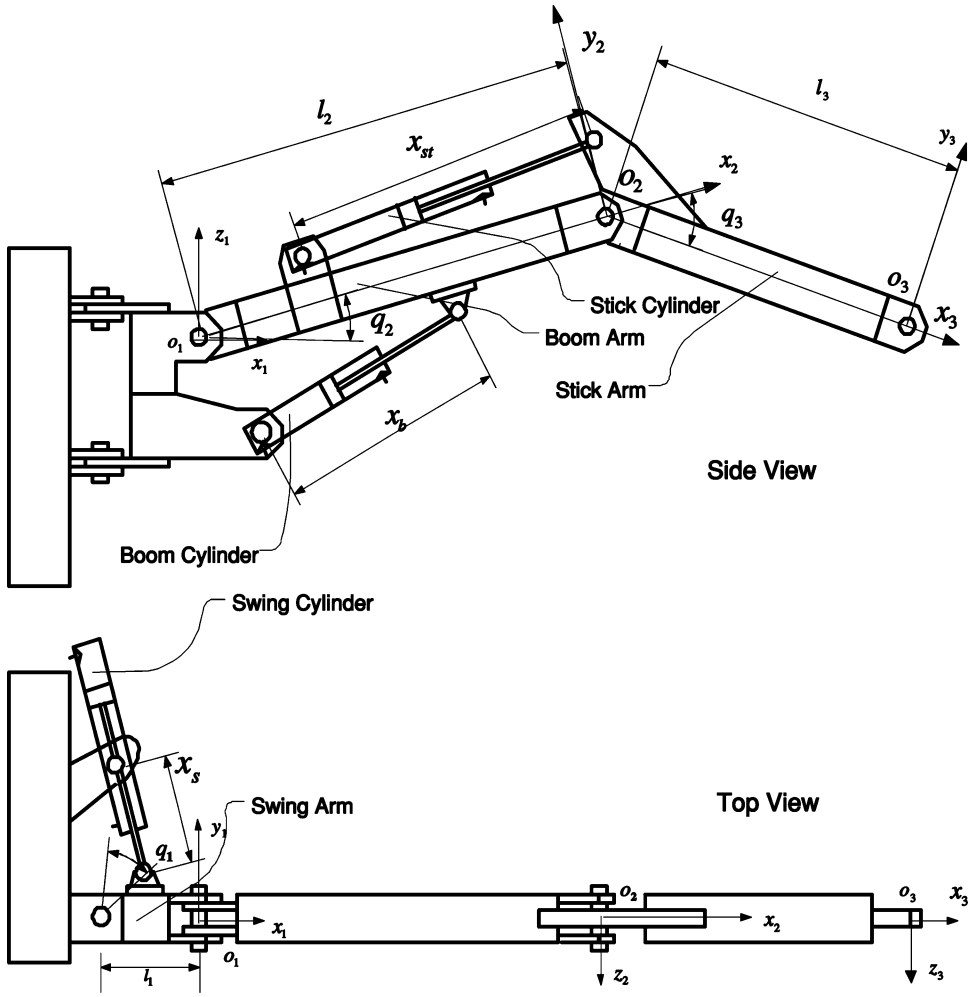

Fig. 3. Three-DOF electro-hydraulic robot arm.

elements of the vectors. With known $\theta_{\min}$ and $\theta_{\max}$, a discontinuous projection $\mathrm{Proj}_{\hat{\theta}}(\bullet) = [\mathrm{Proj}_{\hat{\theta}_1}(\bullet_1), \ldots, \mathrm{Proj}_{\hat{\theta}_n}(\bullet_n)]^T$ can be defined [19], [9] as

$$\mathrm{Proj}_{\hat{\theta}_i}(\bullet_i) = \begin{cases} 0, & \text{if } \hat{\theta}_i = \theta_{i\max} \text{ and } \bullet_i > 0 \\ 0, & \text{if } \hat{\theta}_i = \theta_{i\min} \text{ and } \bullet_i < 0 \\ \bullet_i, & \text{otherwise.} \end{cases} \tag{6}$$

By using an adaptation law given by

$$\dot{\hat{\theta}} = \mathrm{Proj}_{\hat{\theta}}(\Gamma\tau) \tag{7}$$

where $\Gamma > 0$ is a diagonal matrix and τ is an adaptation function to be synthesized later, it can be shown [27] that for any adaptation function τ, the projection mapping used in (7) guarantees

$$\begin{aligned} &\text{(P1)} \quad \hat{\theta} \in \bar{\Omega}_\theta \triangleq \{\hat{\theta} : \theta_{\min} \le \hat{\theta} \le \theta_{\max}\} \\ &\text{(P2)} \quad \tilde{\theta}^T(\Gamma^{-1}\mathrm{Proj}_{\hat{\theta}}(\Gamma\tau) - \tau) \le 0, \ \forall \tau. \end{aligned} \tag{8}$$

Unless explicitly specified, the adaptation law structure (7) with the discontinuous projection (6) will be used wherever adaptation is needed.

IV. Nonlinear Cartridge Valve Flow Mapping

For controller design purpose, one needs an accurate yet simple model for the cartridge valves. Although the cartridge valve has simple structure, the precise mathematical model of its dynamics is very complex and may not be suitable for controller design purpose [6], [13], [15], [22]. Due to the fast response of cartridge valves, it is reasonable to neglect the dynamics from the commanded input voltage to the orifice opening. With this simplification, x_{vi} is related to the valve command voltage u_{vi} by a static mapping. Thus, from (5)

$$Q_{vi} = f_{vi}(\Delta P_{vi}, u_{vi}), \quad i = 1, 2, \ldots, 5 \tag{9}$$

where f_{vi} are some nonlinear functions. Though analytical forms of the above equations may not be known, one can always use experimentally obtained flow mapping lookup tables to approximate the above functions. Fig. 4 shows one of the five flow mappings, i.e., the nonlinear flow rate through a cartridge valve as a function of the valve input voltage and the pressure drop across the valve orifice. As seen, the flow mappings have deadbands and complex shapes that cannot be described by simple analytical nonlinear functions like those used in traditional valves. The previous flow mapping plots can be inverted to give the valve input voltage as the function

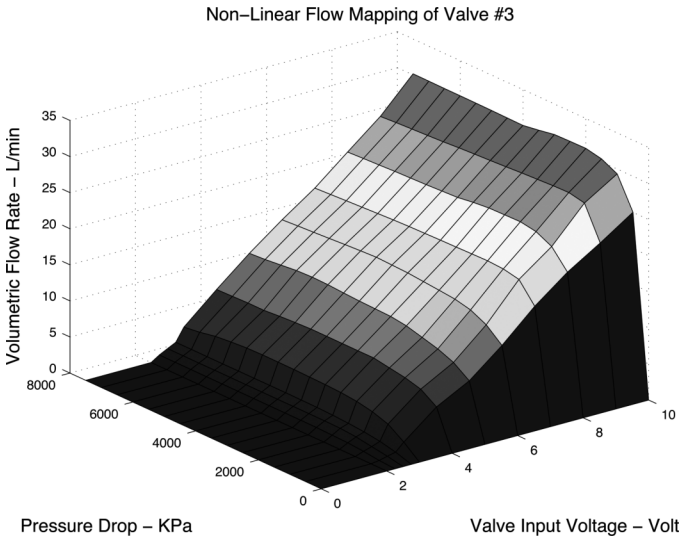

Fig. 4. Experimentally obtained flow mapping of Valve #3.

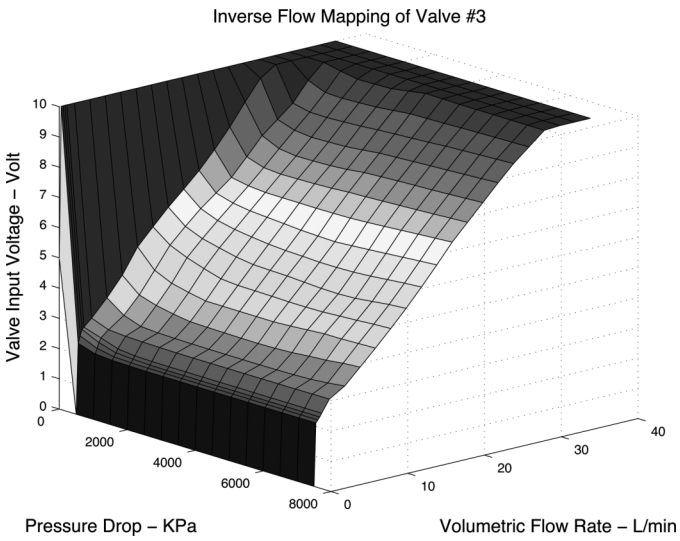

Fig. 5. Inverse flow mapping of Valve #3.

of the flow rate and the pressure drop. The resulting inverse flow mapping, as shown in Fig. 5, will be used to calculate the control signals once given the flow rates that the valves have to provide.

As the experiments to obtain the previous flow mappings can only be done with finite number of sample points, there might be quite substantial flow modeling errors. As such, the Q_1 and Q_2 in (3) should be expressed as

$$\begin{aligned} Q_1 &= Q_{1M} + \tilde{Q}_1 \\ Q_2 &= Q_{2M} + \tilde{Q}_2 \end{aligned} \tag{10}$$

where Q_{1M} and Q_{2M} represent the flows obtained from the previous valve flow mappings and $\tilde{Q}_1$ and $\tilde{Q}_2$ represent the modeling errors of the flow mappings. The effect of the flow modeling errors will be dealt with through robust feedback in the controller design stage.

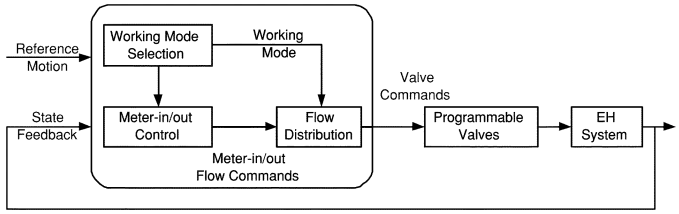

Fig. 6. Two-level control structure.

V. Two-Level Coordinated Control Strategy

The difficulties in the coordinate control of the five cartridge valves for simultaneous precise motion tracking and pressure control for energy saving are to be dealt with through a two-level controllers, as illustrated in Fig. 6. Given the current system states and desired motion trajectory, the task level controller determines the configurations of the programmable valves that would enable significant energy saving while without losing hydraulic circuit controllability for precise motion tracking, which is referred to as the working mode selection. Under the selected working mode, the valve level controller uses the adaptive robust control technique to control the pressures in both chambers independently to achieve the stated dual objectives. The details are given as follows.

A. Working Mode Selection

Let $P_L = P_1A_1 - P_2A_2$ be the load force to actuate the cylinder rod. For precise motion tracking, one needs to control P_L accurately to deliver the desired load force that can generate the required motion. With conventional four-way valves, the solution is unique because the two chamber pressures P_1 and P_2 are coupled and cannot be controlled independently. However, with the programmable valves, the solution is no longer unique. The fact that both P_1 and P_2 can be controlled independently results in tremendous flexibility to control the system. The solution pursued in this paper is to regulate P_L to track the desired motion trajectory while maintain P_1 and P_2 as low as possible for energy saving. Thus, one of the two cylinder chambers will be kept at a low pressure, which is referred to as the offside, while the other chamber's pressure would be critical to the motion tracking and is referred to as working side in the following.

In the hydraulic industry the working mode selection is normally done based on the directions of the load and the desired motion only; for example, the overrunning load in which the load is in the same direction as the desired motion and the resistive load in which the load is opposite to the direction of the desired motion. This *ad hoc* method may be adequate during the steady-state period of the system but not for transient periods such as the rapid acceleration or deceleration periods. For example, during the acceleration period, it may still need large external hydraulic energy to achieve the required acceleration even with an overrunning load. To overcome these transient problems of traditional *ad hoc* working mode selection methods, this paper will present a nonlinear model based one. Specifically, instead of simply checking the load and motion directions to make the working mode selection, the proposed method first calculates the desired force of the hydraulic cylinder that is needed to deliver the required motion and uses this information along

TABLE I
PROGRAMMABLE VALVES TRACKING MODE SELECTION

$\dot{x}_d$	P_{lda}	Valve Configuration	Off-side	Mode
>0	>0	$Q_1 = Q_{v2}$ $Q_2 = Q_{v5}$	P_2	T1
>0	<0	$Q_1 = Q_{v2} - Q_{v3}$ $Q_2 = -Q_{v3}$	P_1	T2
<0	>0 $P_1 > P_2$	$Q_1 = -Q_{v3}$ $Q_2 = Q_{v5} - Q_{v3}$	P_2	T3
<0	>0 $P_1 \leq P2$	$Q_1 = -Q_{v1}$ $Q_2 = -Q_{v4}$	P_2	T4
<0	<0	$Q_1 = -Q_{v1}$ $Q_2 = -Q_{v4}$	P_1	T5

TABLE II
PROGRAMMABLE VALVES REGULATION MODE SELECTION

$\dot{x}_d$	$x - x_d$	Valve Configuration	Off-side	Mode
$=0$	$>\varepsilon$	$Q_1 = -Q_{v3}$ $Q_2 = Q_{v5} - Q_{v3}$	P_2	R1
$=0$	$<-\varepsilon$	$Q_1 = Q_{v2}$ $Q_2 = Q_{v5}$	P_2	R2
$=0$	*otherwise*	$Q_1 = 0$ $Q_2 = 0$		R3

with the desired motion and actual chamber pressure measurement to determine how the five cartridge valves should be used. The calculation of the desired load force will be explained in detail in Section V-C.

The working mode selection is task dependent. There are five tracking modes and three regulation modes proposed in this research. The tracking mode selection, shown in Table I, is based on the desired cylinder velocity $\dot{x}_d$, the actual cylinder pressures P_1 and P_2, and the desired load force P_{Lda} for motion tracking; the detailed expression of P_{Lda} will be given later in the motion controller design subsection. The regulation mode selection is shown in Table II, where ε is a small preset positive number.

Mode $T1$ represents the standard working condition, in which the control command calls for the cylinder to be extended with a resistive load. The most efficient usage of the programmable valves is to use valve number 2 to provide the control flow Q_1 for the head end chamber and to use the valve number 5 to maintain a low pressure P_2 in the rod end chamber, i.e., the offside.

In mode $T2$, the cylinder may extend under an external overrunning force or in a deceleration period, and $P_2 > P_1$, which enables the regeneration flow from rod end chamber to head end chamber. This reduces the flow needed from the pump and, thus, saving energy significantly. Flow from the pump is still needed due to the large head end area. In this case, valve number 3 is used to control the cylinder motion and valve number 2 is used to maintain the desired low pressure in the offside, the head end chamber.

Mode $T5$ is another standard operation in that the cylinder is to be retraced under a resistive load. Valve number 4 is used to provide the control flow while valve number 1 is used to maintain the head end pressure at low level.

Mode $T4$ is used in the situation that the cylinder is to be retracted under an overrunning external force or in a deceleration period, but the head end pressure P_1 is not higher than the rod end pressure P_2. In this mode, valve number 1 is used to control the cylinder motion and valve number 4 is used to regulate the rod end pressure to the desired low level.

Mode $T3$ occurs under the similar condition as T4, with the additional constraint that $P_1 > P_2$, which ensures that the regeneration flow can be pumped from the head end chamber to the rod end chamber through valve number 3. The excess flow due to the larger head end area is drained back to the tank through valve number 5. In this mode, valve number 3 is used to control cylinder motion while valve 5 to regulate the desired low pressure at rod end chamber. This results an operation requiring no pump flow and no active energy usage.

When the desired velocity is zero, the cylinder is working in a position regulation mode. Potential energy can be used to lower the cylinder/arm in mode $R1$, which is similar to mode $T3$. No regeneration flow is expected to use in mode $R2$, which is similar to mode $T5$. The small positive number ε is the preset tolerance. When the position difference between the actual and desired positions is less than the tolerance, the system enters mode $R3$ and would close all the valves.

B. Offside Adaptive Robust Pressure Regulator Design

The objective of the offside pressure regulator is to keep the offside pressure at a constant low pressure P_0. To illustrate the design procedure, this section designs a pressure regulator for those working modes, for which P_2 is the offside. The pressure regulator design for P_1 follows the same procedure and is omitted here.

The dynamics of P_2 is described in (3) and (10). In order to use parameter adaptation to reduce parametric uncertainties to improve performance, it is necessary to linearly parameterize the system dynamics in terms of a set of unknown parameters θ_p. θ_p is defined as $\theta_p = [\theta_\beta, \theta_Q]^T$, where $\theta_\beta = \beta_e$ and $\theta_Q = \beta_e \tilde{Q}_{2n}$, in which $\tilde{Q}_{2n}$ is the nominal value of $\tilde{Q}_2$. The P_2 dynamics can then be rewritten as follows:

$$\dot{P}_2 = \frac{A_2}{V_2}\frac{\partial x_L}{\partial q_2}\dot{q}_2\theta_\beta - \frac{\theta_\beta}{V_2}Q_{2M} - \frac{\theta_Q}{V_2} + \Delta_{Q2} \tag{11}$$

where $\Delta_{Q2} = (\beta_e)/(V_2)(\tilde{Q}_{2n} - \tilde{Q2})$. The goal is to have the cylinder pressure regulated to a desired constant low pressure P_0. Assume that the parameters are bounded by some known bounds, and so is Δ_{Q2}. This assumption is realistic because both bulk modulus β_e and the modeling error of the flow mapping are practically bounded.

Define the pressure regulation error as $e_{p2} = P_2 - P_0$, the error dynamics would be the same as the pressure dynamics because P_0 is constant

$$\dot{e}_{P2} = -\frac{\theta_\beta}{V_2}Q_{2M} + \frac{A_2}{V_2}\frac{\partial x_L}{\partial q_2}\dot{q}_2\theta_\beta - \frac{\theta_Q}{V_2} + \Delta_{Q2}. \tag{12}$$

With Q_{2M} being the control input, the proposed control law is given by

$$\begin{aligned} Q_{2M} &= Q_{2Ma} + Q_{2Ms} \\ Q_{2Ma} &= A_2\frac{\partial x_L}{\partial q_2}\dot{q}_2 - \frac{\hat{\theta}_Q}{\hat{\theta}_\beta} \\ Q_{2Ms} &= (k_{p2} + k_{p2s})\frac{V_2}{\theta_{\beta\min}}e_{p2} \end{aligned} \tag{13}$$

where Q_{2ma} is the model compensation term and Q_{2Ms} is a robust feedback term, in which $k_{p2} > 0$ and k_{p2s} is a nonlinear feedback gain chosen to satisfy the following condition for performance robustness to model uncertainties:

$$\begin{aligned} &(i) \quad e_{p2}\left(-k_{p2s}\frac{\theta_\beta}{\theta_{\beta\min}}e_{p2}+\phi_{p2}^T\tilde{\theta}_{p2}-\Delta_{Q2}\right)\le\varepsilon_p \\ &(ii) \quad -k_{p2s}\frac{\theta_\beta}{\theta_{\beta\min}}e_{p2}^2\le 0 \end{aligned} \tag{14}$$

where $\phi_{p2} = [(A_2)/(V_2)(\partial x_L)/(\partial q_2)\dot{q}_2 - (Q_{2Ma})/(V_2), -(1/V_2)]^T$. The parameter adaptation law is defined in (7) with a positive definite diagonal adaptation rate matrix Γ_p and an adaptation function defined as

$$\tau_p = \phi_{p2}\cdot e_{p2}. \tag{15}$$

C. Working-Side Adaptive Robust Motion Controller Design

The dynamics of the boom motion and cylinder pressures were described in (2) and (3). Define a set of parameters as $\theta = [\theta_1,\ldots,\theta_6]^T$, $\theta_1 = (1)/(1+(l_e^2)/(J_c)m_L)$, $\theta_2 = (D_f)/(J_c + m_L l_e^2)$, $\theta_3 = (T_n)/(J_c + m_L l_e^2)$, $\theta_4 = \beta_e$, $\theta_5 = \beta_e\tilde{Q}_{1n}$, and $\theta_6 = \beta_e\tilde{Q}_{2n}$, in which T_n, $\tilde{Q}_{1n}$, and $\tilde{Q}_{2n}$ represent the nominal values of T, $\tilde{Q}_1$, and $\tilde{Q}_2$, respectively. The system dynamic equations can thus be rewritten as

$$\begin{aligned} \ddot{q}_2 &= \frac{\theta_1}{J_c}\left[\frac{\partial x_L}{\partial q_2}(P_1A_1-P_2A_2)-G_c\right]+\frac{\theta_1}{l_e^2}gl_g \\ &\quad -\dot{q}_2\theta_2+\theta_3-\frac{1}{l_e^2}gl_g+\Delta \\ \dot{P}_1 &= -\frac{A_1}{V_1}\frac{\partial x_L}{\partial q_2}\dot{q}_2\theta_4+\frac{\theta_4}{V_1}Q_{1M}+\frac{\theta_5}{V_1}+\Delta_{Q1} \\ \dot{P}_2 &= \frac{A_2}{V_2}\frac{\partial x_L}{\partial q_2}\dot{q}_2\theta_4-\frac{\theta_4}{V_2}Q_{2M}-\frac{\theta_6}{V_2}+\Delta_{Q2} \end{aligned} \tag{16}$$

where $\Delta = -(1)/(J_c + m_L l_e^2)(T_n - T)$, $\Delta_{Q1} = (\beta_e)/(V_1)(\tilde{Q}_{1n} - \tilde{Q}_1)$, and $\Delta_{Q2} = (\beta_e)/(V_2)(\tilde{Q}_{2n} - \tilde{Q}_2)$.

To illustrate the adaptive robust motion controller design, this section presents a design procedure for those working modes whose working side is the head end chamber, i.e., P_1. The controller design for P_2 to be the working side follows the same procedure and is omitted here.

Step 1: Define a switching-function-like quantity as

$$z_2 = \dot{z}_1 + k_1 z_1 = \dot{q}_2 - \dot{q}_{2r}, \quad \dot{q}_{2r} \triangleq \dot{q}_d - k_1 z_1 \tag{17}$$

where $z_1 = q_2 - q_d(t)$ is the output tracking error with $q_d(t)$ being the reference trajectory. Differentiate (17) while noting (16)

$$\begin{aligned} \dot{z}_2 &= \theta_1\left[\frac{1}{J_c}\left(\frac{\partial x_L}{\partial q_2}P_L-G_c\right)+\frac{1}{l_e^2}gl_g\right]-\frac{1}{l_e^2}gl_g \\ &\quad -\ddot{q}_{2r}-\theta_2\dot{q}_2+\theta_3+\Delta \end{aligned} \tag{18}$$

where $P_L = P_1A_1 - P_2A_2$ is defined as the load force. If we treat P_L as the control input to (18), we can synthesize a virtual control law P_{Ld} such that z_2 is as small as possible. Since (18) has both parametric uncertainties θ_1 through θ_3 and uncertain nonlinearity Δ, the ARC approach proposed by Yao [24] is generalized to deal with these model uncertainties effectively. The resulting control function P_{Ld} consists of two parts given by

$$\begin{aligned} P_{Ld}(q_2,\dot{q}_2,\hat{\theta}_1,\hat{\theta}_2,t) &= P_{Lda}+P_{Lds} \\ P_{Lda} &= \frac{\partial q_2}{\partial x_L}\left[G_c+\frac{J_c}{\hat{\theta}_1}\left(-\frac{\hat{\theta}_1}{l_e^2}gl_g+\hat{\theta}_2\dot{q}_2\right.\right. \\ &\quad \left.\left.-\theta_3+\frac{1}{l_e^2}gl_g+\ddot{q}_{2r}\right)\right] \\ P_{Lds} &= P_{Lds1}+P_{Lds2} \\ P_{Lds1} &= -\frac{J_c}{\theta_{1\min}}\frac{\partial q_2}{\partial x_L}k_2z_2 \end{aligned} \tag{19}$$

in which P_{Lda} functions as an adaptive model compensation, and P_{Lds} is a robust control law with $k_2 > 0$, and P_{Lds2} is chosen to satisfy the following robust performance conditions as in [25]:

$$\begin{aligned} &\text{(i)} \quad z_2\left[\frac{1}{J_c}\theta_1\frac{\partial x_L}{\partial q_2}P_{Lds2}-\tilde{\theta}^T\phi_2+\Delta\right]\le\epsilon_2 \\ &\text{(ii)} \quad z_2\frac{\partial x_L}{\partial q_2}P_{Lds2}\le 0 \end{aligned} \tag{20}$$

where ϵ_2 is a design parameter. If P_L were the actual control input, the adaptation function as defined in [5] would be

$$\begin{aligned} \tau_2 &= \phi_2 z_2 \\ \phi_2 &\triangleq \left[\frac{1}{J_c}\left(\frac{\partial x_L}{\partial q_2}P_{Lda}-G_c\right)+\frac{1}{l_e^2}gl_g,-\dot{q}_2,1,0,0,0\right]^T \end{aligned} \tag{21}$$

Step 2: Let $z_3 = P_L - P_{Ld}$ denote the input discrepancy. In this step, a virtual control flow will be synthesized so that z_3 converges to zero or a small value with a guaranteed transient performance and accuracy.

From (16)

$$\begin{aligned} \dot{z}_3 &= \dot{P}_L-\dot{P}_{Ld} \\ &= -\left(\frac{A_1^2}{V_1}+\frac{A_2^2}{V_2}\right)\frac{\partial x_L}{\partial q_2}\dot{q}_2\theta_4+\frac{A_2}{V_2}\theta_4Q_{2M}+\frac{A_1}{V_1}\theta_5+\frac{A_2}{V_2}\theta_6 \\ &\quad -\dot{P}_{Ldc}+\frac{A_1}{V_1}\theta_4Q_{1M}+A_1\Delta_{Q1}-A_2\Delta_{Q2}-\dot{P}_{Ldu} \end{aligned} \tag{22}$$

where

$$\begin{aligned} \dot{P}_{Ldc} &= \frac{\partial P_{Ld}}{\partial q_2}\dot{q}_2+\frac{\partial P_{Ld}}{\partial\dot{q}_2}\hat{\ddot{q}}_2+\frac{\partial P_{Ld}}{\partial t} \\ \dot{P}_{Ldu} &= \frac{\partial P_{Ld}}{\partial\dot{q}_2}\left[-\frac{\tilde{\theta}_1}{J_c}\left(\frac{\partial x_L}{\partial q_2}P_L-G_c\right)\right. \\ &\quad \left.-\frac{\tilde{\theta}_1}{l_e^2}gl_g(q_2)+\tilde{\theta}_2\dot{q}_2-\tilde{\theta}_3+\Delta\right]+\frac{\partial P_{Ld}}{\partial\hat{\theta}}\dot{\hat{\theta}} \end{aligned} \tag{23}$$

in which $\hat{\ddot{q}}_2$ represent the calculable part of $\ddot{q}_2$ given by

$$\hat{\ddot{q}}_2 = \frac{\hat{\theta}_1}{J_c}\left[\frac{\partial x_L}{\partial q_2}P_L-G_c\right]+\frac{\hat{\theta}_1}{l_e^2}gl_g-\hat{\theta}_2\dot{q}_2+\hat{\theta}_3-\frac{1}{l_e^2}gl_g. \tag{24}$$

In (23), $\dot{P}_{Ldc}$ is calculable and can be used in the construction of control functions, but $\dot{P}_{Ldu}$ cannot due to various uncertainties.

Therefore, $\dot{P}_{Ldu}$ has to be dealt with via certain robust feedback in this step design.

In viewing (22), Q_{1M} can be thought as the control input for (22) and step 2 is to synthesize a control function Q_{1Md} for Q_{1M} such that P_L tracks the desired control function P_{Ld} synthesized in Step 1 with a guaranteed transient performance. Similar to (19), the control function Q_{1Md} consists of two parts given by

$$\begin{aligned}
&Q_{1Md}(q_2,\dot{q}_2,P_1,P_2,\hat{\theta},t)\\
&=Q_{1Mda}+Q_{1Mds}\\
&Q_{1Mda}\\
&=\frac{V_1}{A_1\hat{\theta}_4}\left[-\frac{\hat{\theta}_1}{J_c}\frac{\partial x_L}{\partial q_2}z_2\right.\\
&\qquad+\hat{\theta}_4\left(\left(\frac{A_1^2}{V_1}+\frac{A_2^2}{V_2}\right)\frac{\partial x_L}{\partial q_2}\dot{q}_2-\frac{A_2}{V_2}Q_{2M}\right)\\
&\qquad\left.-\hat{\theta}_5\frac{A_1}{V_1}-\hat{\theta}_6\frac{A_2}{V_2}+\dot{P}_{Ldc}\right]\\
&Q_{1Mds}\\
&=Q_{1Mds1}+Q_{1Mds2},\ Q_{1Mds1}=-\frac{V_1}{A_1\theta_{4\min}}k_3z_3 \qquad (25)
\end{aligned}$$

where $k_3>0$. Like (20), Q_{1Mds2} is a robust control function chosen to satisfy the following two robust performance conditions:

$$\begin{aligned}
&\text{(i) } z_3\left[\theta_4Q_{1Mds2}-\tilde{\theta}^T\phi_3-\frac{\partial P_{Ld}}{\partial\dot{q}_2}\Delta+A_1\Delta_{Q_1}-A_2\Delta_{Q_2}\right]\le\epsilon_3\\
&\text{(ii) } z_3Q_{1Mds2}\le 0 \qquad (26)
\end{aligned}$$

where ϵ_3 is a positive design parameter. The adaptation function would be

$$\tau=\tau_2+\phi_3z_3 \qquad (27)$$

where ϕ_3 is defined as

$$\phi_3\triangleq\begin{bmatrix}\frac{1}{J_c}\frac{\partial x_L}{\partial q_2}z_2-\frac{\partial P_{Ld}}{\partial\dot{q}_2}\left[\frac{1}{J_c}\left(\frac{\partial x_L}{\partial q_2}P_L-G_c\right)+\frac{1}{l_e^2}gl_g\right]\\ \frac{\partial P_{Ld}}{\partial\dot{q}_2}\dot{q}_2\\ -\frac{\partial P_{Ld}}{\partial\dot{q}_2}\\ -\left(\frac{A_1^2}{V_1}+\frac{A_2^2}{V_2}\right)\frac{\partial x_L}{\partial q_2}\dot{q}_2+\frac{A_2}{V_2}Q_{2M}+\frac{A_1}{V_1}Q_{1Ma}\\ \frac{A_1}{V_1}\\ \frac{A_2}{V_2}\end{bmatrix}. \qquad (28)$$

D. Flow Distribution and Control Signal Calculation

Once the desired supply and return flow rates Q_{1Md} and Q_{2Md} are synthesized as given in (25) and (13), one needs to distribute the desired flow commands to the five cartridge valves and calculate the control signal for each valve.

The relationships between the supply and return flow rates and the flow rates of the five cartridge valves are described in (4). There seems no unique solution because there are five unknowns and only two equations. However, one can find out by checking the working mode selection Table I and Table II that only two cartridge valves are open while the other three are closed in all working modes. Therefore, the desired supply and return flow rates can be easily distributed to the five cartridge valves uniquely. For example, when the system is working in $T3$ mode, valve #3 and valve #5 are selected and the other three valves are shut off. From Table I, the control flow commands for the valve #3 and valve #5 are then given by $Q_{v3}=-Q_{1Md}$ and $Q_{v5}=Q_{2Md}-Q_{1Md}$, while the flow commands for the other three valves are set to zero, i.e., $Q_{vi}=0\ i=1,2,4$.

The valve control input can then be obtained by checking the inverse flow mapping, such as the one in Fig. 5, which is a lookup table describing the valve input signal as a function of pressure drop across the valve and flow rate through the valve.

VI. Theoretical Control Performance

Theorem 1: With the adaptive robust control law (13) and the projection type adaptation law structure (7) with adaptation function (15) for θ_β, the following results hold.

A) In general, the offside pressure regulation is stable with a prescribed transient performance and accuracy quantified by

$$e_{p_2}^2(t)\le e_{p_2}^2(0)\cdot\exp(-2k_{p_2}t)+\frac{\varepsilon_p}{k_{p_2}}\cdot[1-\exp(-2k_{p_2}t)]. \qquad (29)$$

B) If after a finite time t_0, $\Delta_{Q2}=0$, i.e., the model uncertainties are due to parametric uncertainties only, in addition to the result in A, asymptotic pressure tracking ($e_{p_2}\to 0$ as $t\to\infty$) is obtained for any positive gain k_{p_2} and ε_p.

Proof: Define a positive definite scalar function $V_p(t)=1/2e_{p2}^2$. Differentiate V_p while noting (13) and (14), one can obtain

$$\begin{aligned}
\dot{V}_p&=e_{p_2}\cdot\dot{e}_{p_2}\\
&=e_{p_2}\left(-\frac{\theta_\beta}{V_2}Q_{2M}+\frac{A_2}{V_2}\frac{\partial x_L}{\partial q_2}\dot{q}_2\theta_\beta-\frac{\theta_Q}{V_2}+\Delta_{Q2}\right)\\
&=-k_{p_2}e_{p_2}^2-e_{p2}\left(k_{p2s}\frac{\theta_\beta}{\theta_{\beta\min}}e_{p2}-\phi_{p2}^T\tilde{\theta}_p+\Delta_{Q2}\right)\\
&\le-k_{p_2}e_{p_2}^2+\varepsilon_p=-2k_{p2}V_p(t)+\varepsilon_p. \qquad (30)
\end{aligned}$$

Therefore

$$V_p\le V_p(0)\cdot\exp(-2k_{p2}t)+\frac{\varepsilon_p}{2k_{p2}}\cdot[1-\exp(-2k_{p2}t)] \qquad (31)$$

which is equivalent to (29).

To prove part B, define a positive definite scalar function $V_{p\theta}(t)=V_p+(1/2)\tilde{\theta}_p^T\Gamma^{-1}\tilde{\theta}_p$. Noting $\Delta_{Q2}=0$ and $\dot{\tilde{\theta}}_p=\dot{\hat{\theta}}_p$, from (15), (P2) of (8), and (14), one can obtain

$$\begin{aligned}
\dot{V}_{p\theta}&=\dot{V}_p+\tilde{\theta}_p\Gamma^{-1}\dot{\hat{\theta}}_p=-k_{p_2}e_{p_2}^2\\
&\quad-e_{p2}\left(k_{p2s}\frac{\theta_\beta}{\theta_{\beta\min}}e_{p2}-\phi_{p2}^T\tilde{\theta}_p\right)+\tilde{\theta}_p\Gamma^{-1}\mathrm{Proj}_{\hat{\theta}}(\Gamma\tau_p)\\
&=-k_{p_2}e_{p_2}^2-k_{p2s}\frac{\theta_\beta}{\theta_{\beta\min}}e_{p2}^2+\tilde{\theta}_p^T[\Gamma^{-1}\mathrm{Proj}_{\hat{\theta}}(\Gamma\tau_p)-\tau_p]\\
&\le-k_{p_2}e_{p_2}^2. \qquad (32)
\end{aligned}$$

Therefore, $e_{p_2} \in L_2^2$. It is also easy to check that $\dot{e}_{p_2}$ is bounded. So, $e_{p_2} \to 0$ as $t \to \infty$ by the Barbalat's lemma.

Theorem 2: With the adaptive robust control law (25) and the projection type adaptation law (7) with adaptation function (27) for θ defined in Section IV-C, the following results hold.

A) In general, the overall closed-loop system is stable with a prescribed transient performance and final tracking accuracy quantified by

$$V_3(t) \le V_3(0) \cdot \exp(-2\lambda t) + \frac{\varepsilon}{2\lambda} \cdot [1 - \exp(-2\lambda t)] \quad (33)$$

where $V_3(t) = 1/2 \sum_{i=2}^{3} k_i z_i^2, \lambda = \min\{k_2,\ k_3\}$ and $\varepsilon = \epsilon_2 + \epsilon_3$.

B) If after a finite time t_0, $\Delta = 0$, and $\Delta_{Qi} = 0\ i = 1,\ 2,$ i.e., the model uncertainties are due to parametric uncertainties only, in addition to the results in A, asymptotic motion tracking ($z_1 \to 0$ as $t \to \infty$) is obtained for any positive gain $k_i,\ k = 1, 2, 3$ and $\varepsilon_i,\ i = 2, 3$.

Proof: Differentiate $V_3(t)$, one can get

$$\begin{aligned}\dot{V}_3 = &-\frac{\theta_1}{\theta_{1\min}} k_2 z_2^2 - k_3 z_3^2 \\ &+ z_2 \left\{ \frac{\theta_1}{J_c} \frac{\partial x_L}{\partial q_2} P_{Lds2} - \tilde{\theta}^T \phi_2 + \Delta \right\} \\ &+ z_3 \left\{ \theta_4 Q_{1Mds2} - \tilde{\theta}^T \phi_3 \right. \\ &\qquad \left. - \frac{\partial P_{Ld}}{\partial \dot{q}_2} \Delta + A_1 \Delta_{Q_1} - A_2 \Delta_{Q_2} \right\} \\ &\le -k_2 z_2^2 - k_3 z_3^2 + \epsilon_2 + \epsilon_3 \le -2\lambda V_3 + \varepsilon \end{aligned} \quad (34)$$

which proves (33).

To prove part B, define a positive definite scalar function $V(t) = V_3 + 1/2 \tilde{\theta}^T \Gamma^{-1} \tilde{\theta}$. Noting all disturbance terms are zero and $\dot{\tilde{\theta}} = \dot{\hat{\theta}}$, from (27), (P2) of (8), one can obtain

$$\begin{aligned}\dot{V} &= \dot{V}_3 + \tilde{\theta}^T \Gamma^{-1} \dot{\hat{\theta}} \\ &\le -\sum_{j=2}^{3} k_j z_j^2 - \frac{\theta_1}{\theta_{1\min}} k_{2s} z_2^2 - k_{3s} z_3^2 \\ &\quad - \tilde{\theta}^T (\phi_2 z_2 + \phi_3 z_3) + \tilde{\theta}^T \Gamma^{-1} \mathrm{Proj}_{\hat{\theta}}(\Gamma \tau) \\ &\le -\sum_{j=2}^{3} k_j z_j^2 + \tilde{\theta}^T [\Gamma^{-1} \mathrm{Proj}_{\hat{\theta}}(\Gamma \tau) - \tau] \\ &\le -\sum_{j=2}^{3} k_j z_j^2. \end{aligned} \quad (35)$$

Therefore, $z \in L_2^2$. It is also easy to check that $\dot{z}_1$ is bounded. So, $z_1 \to 0$ as $t \to \infty$ by the Barbalat's lemma.

VII. Implementation and Experiments

The conditions for the robust control functions, i.e., inequalities (14), (20), and (26), share the same format as in the following equation, which leads to the following practical means to implement these functions:

$$\begin{aligned} &\text{(i)} \quad z[\beta_\theta \alpha_s - \tilde{\theta}^T \phi + \tilde{d}] \le \epsilon \\ &\text{(ii)} \quad z \beta_\theta \alpha_s \le 0 \end{aligned} \quad (36)$$

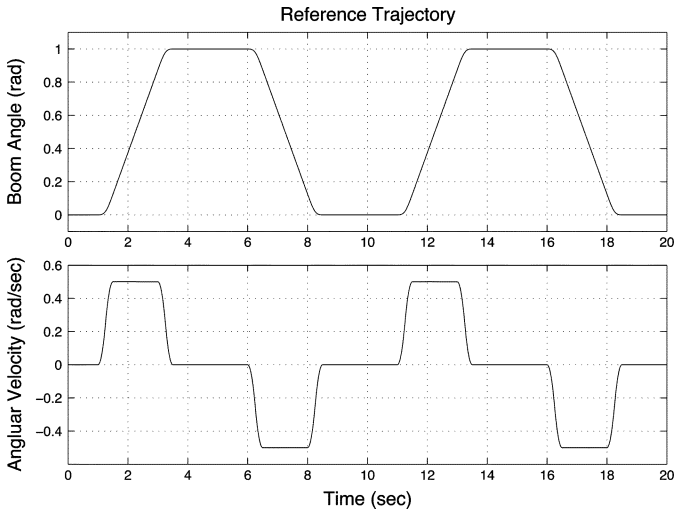

Fig. 7. Point-to-point desired trajectory.

where z is the tracking error, β_θ is an unknown positive scalar, $\tilde{\theta}$ is the parameter estimation error, ϕ is the regressor vector, $\tilde{d}$ represents all unknown nonlinearities that are assumed to be bounded by δ_d, and ϵ is a design parameter which can be arbitrarily small. Essentially, condition (i) shows the robust control function α_s is synthesized to dominate the model uncertainties including both parametric uncertainties $\tilde{\theta}$ and uncertain nonlinearities $\tilde{d}$; condition (ii) guarantees that α_s is dissipating in nature so that it does not interfere with the functionality of the adaptive control part. The existence of such robust control function and how to choose the robust control function to satisfy the two conditions can be found in [24], [28], and [29]. One example of smooth α_s function satisfying (36) can be chosen as [28]

$$\alpha_s = -\frac{h}{2\beta_{\theta\min}\epsilon} z, \quad h \ge \|\theta_{\max} - \theta_{\min}\|^2 \|\phi\|^2 + \delta_d^2. \quad (37)$$

The previous procedure to select the robust control functions to satisfy (14), (20), and (26) is rigorous and should be the formal approach to choose. However, it increases the complexity of the resulting control law considerably since it may need a significant amount of computation time to calculate them and their partial derivatives during the backstepping designs. As an alternative, a pragmatic approach is to simply choose k_{p2}, k_2, and k_3 large enough without worrying about the specific values of k_{p2s}, k_{2s}, and k_{3s}. By doing so, (14), (20), and (26) will be satisfied at least locally for some ϵ around the desired trajectory, which is done in the following experiments. Furthermore, the larger k_{p2}, k_2, and k_3 are the smaller ϵ.

Experiments were done to test the proposed two-level control system. The programmable valves were used to control the boom motion of the electro-hydraulic arm to track a desired motion trajectory, as shown in Fig. 7. The programmable valves were compared with a critical center servo valve and a closed-center PDC valve with deadband compensation in terms of both control performance as well as energy usage. Similar ARC controllers were designed for the servo valve and PDC valve with the servo valve and the PDC valve modeled by the

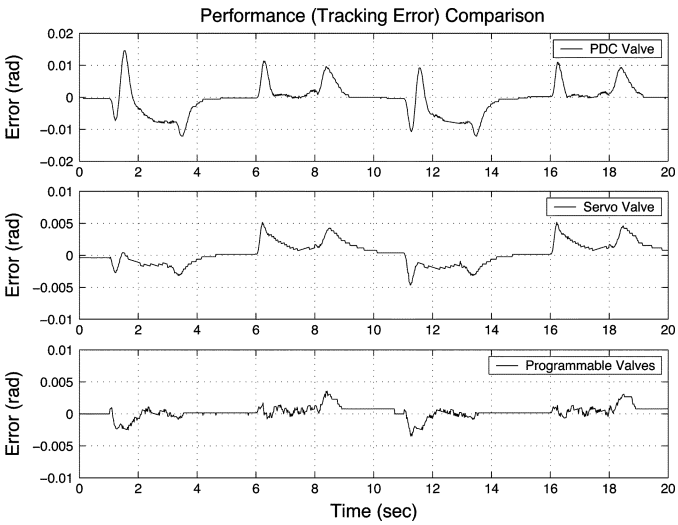

Fig. 8. Comparison of tracking performance.

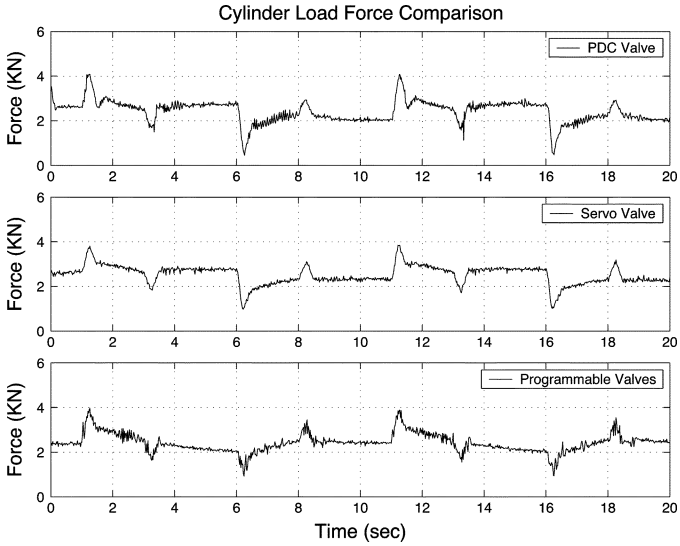

Fig. 9. Comparison of cylinder load force.

TABLE III
COMPARISON OF TRACKING ERRORS

Valve	$\|e\|_1$	$\|e\|_2$	$\|e\|_\infty$
PDC	0.0030	0.0046	0.0146
Servo	0.0014	0.0018	0.0051
Programmable	0.0007	0.0010	0.0036

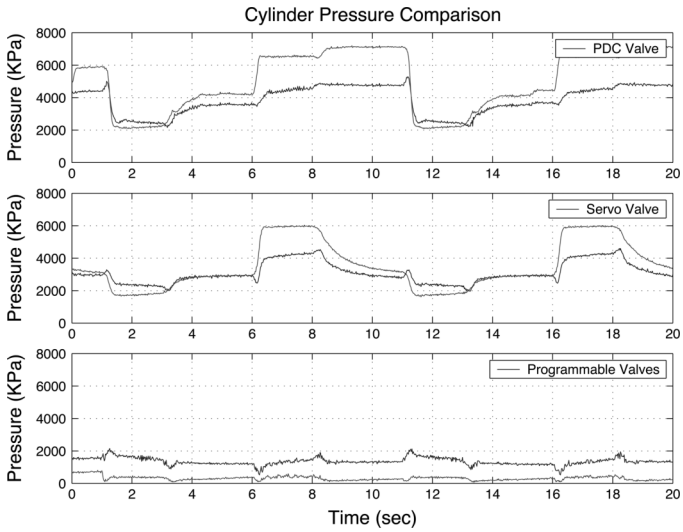

Fig. 10. Comparison of cylinder pressures.

orifice flow equations that have been widely used in fluid power industry [25].

The tracking performances of the three systems for the same desired motion trajectory shown in Fig. 7 were plotted in Fig. 8. Both the servo valve and the programmable valves showed excellent tracking performance; noting the larger scale used for the plot of the PDC valve tracking error. It is also shown that the closed-loop control performance of the overall system with the proposed programmable valves is at least, if not better, the same level as that of using the expensive servo valve. Keeping in mind that the low-cost cartridge valves used in the proposed programmable valves are traditionally labeled as low accuracy valves and have never been used in precision hydraulics, the practical significance of the proposed advanced controls with programmable valves becomes self-evident. A more detailed comparison of tracking errors was given in Table III, where the tracking errors were defined as follows: 1) $\|e\|_1$ is defined as $\int_0^{20} |e(t)|d(t)$; 2) $\|e\|_2$ is defined as $\int_0^{20} e^2(t)d(t)$; and 3) $\|e\|_\infty$ is defined as $\max|e(t)|$.

A comparison of cylinder forces of the three systems was given in Fig. 9. The cylinder forces were calculated by $P_1A_1 - P_2A_2$. Because all three systems tracked the same desired motion trajectory well, as expected, the cylinder force profiles were similar.

Though the three systems have similar cylinder force profiles, the pressures of each system were quite different, as shown in Fig. 10. The cylinder pressures in the system controlled by the proposed programmable valves were much lower than the pressures in the other two systems, with one pressure always close to the tank pressure—a preset pressure of 200 KPa to compensate for line loss and to prevent cavitation. This was the result of decoupled and independent control of cylinder pressures that were made possible by the proposed programmable valves.

The power usages of the three systems were shown in Fig. 11. The experiment setup used a pump with a constant supplied pressure of 6900 KPa (1000 PSI). The power was calculated as the product of supply pressure and pump flow rate that was used during the motion. As seen, during the upward motion periods (roughly, 1–3.5 s and 11–13.5 s), the three systems used almost the same amount of energy as active pump energy is needed to lift the payload. However, during the downward motion periods (roughly, 6–8.5 s and 16–18.5 s), the programmable valves controlled system did not use any pump energy at all due to the use of regeneration flow for precise cylinder motion control, while the other two systems still needed pump energy for a controlled downward motion. It is noted that the proposed programmable valves not only enable the use of regeneration flow for energy saving, but also the precise control of regeneration flow for a well controlled motion—the resulting motion tracking

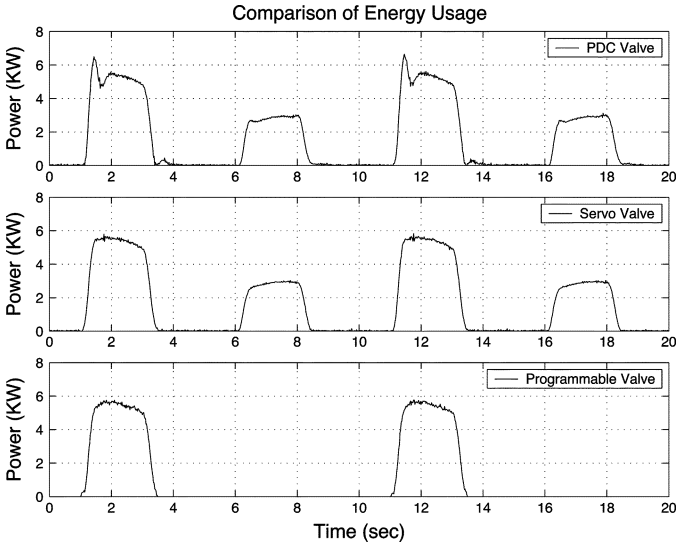

Fig. 11. Comparison of energy usage with constant pressure pump.

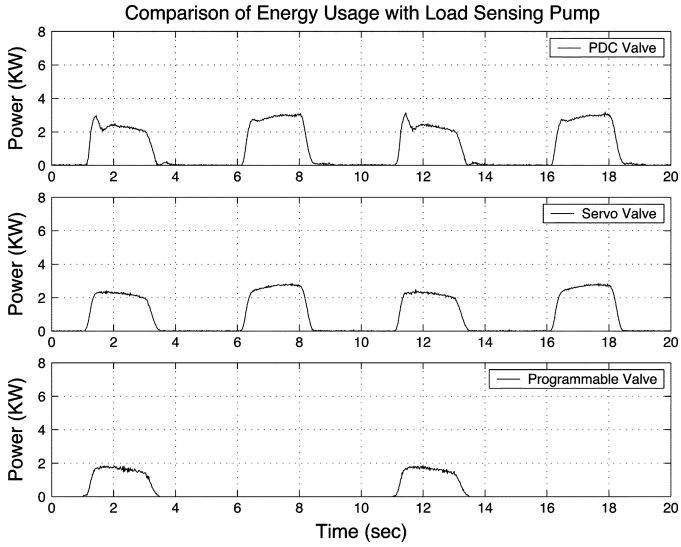

Fig. 12. Comparison of energy usage with load sensing pump.

TABLE IV
COMPARISON OF ENERGY USAGE

Valve	Constant Pressure Pump	Load Sensing Pump
PDC	32.4KJ	20.9KJ
Servo	32.7KJ	19.3KJ
Programmable	21.3KJ	6.4KJ

error shown in Fig. 8 is even better than that is achieved by a servo valve. Such a use of regeneration flow is much different from existing energy saving systems [2], [8], where the regeneration flow cannot be precisely controlled and, subsequently, only free drop motion, not any controlled motion, can be obtained. The total pump energy used by three systems for this specific task was shown in the second column of Table IV. The programmable valves controlled system used about 2/3 of the energy consumed by the other systems.

In mobile hydraulic industry, instead of a constant supplied pressure pump, a load sensing pump (i.e., the supplied pressure of the pump is varied according to the required cylinder chamber pressures) is normally used for further energy saving [2]. When a load sensing pump is used together with the proposed programmable valves, much more energy saving can be obtained due to the significantly reduced cylinder working pressures as shown in Fig. 10. Unfortunately, our experimental setup did not have a load sensing pump and it was impossible to experimentally show the energy saving with a load sensing pump. Instead, a virtual comparison was done to mimic a load sensing pump by adding 500 KPa to the cylinder working pressure connected to the pump as the pump supplied pressure. With this assumption, the comparison results for pump power usage of three systems were shown in Fig. 12 with the total energy usages shown in the third column of Table IV. As seen, further energy saving was obtained by the programmable valves due to the low cylinder working pressures. The programmable valve controlled system used about only 1/3 of the energy consumed by the other two systems.

VIII. CONCLUSION

A two-level coordinated control system was proposed and experimentally tested to make full use of the hardware flexibility offered by the proposed programmable valves in meeting the dual objectives of precision motion tracking and significant energy saving of electro-hydraulic systems. The task-level controller selects the working mode to coordinate the five cartridge valves for a proper hydraulic circuitry. The valve-level controller utilizes the advanced ARC technique to guarantee a prescribed closed-loop control performance even in the presence of large parameter variations and external disturbances. Comparatively experimental results obtained show that the dual objectives of energy saving and precision motion control have been achieved with the proposed intelligent integration of advanced control techniques (i.e., ARC motion and pressure control designs) and novel hardware redesigns (i.e., the use of the proposed programmable valves for hydraulic systems).

REFERENCES

[1] J. A. Aardema, "Hydraulic circuit having dual electrohydraulic control valves," U. S. Patent 5 568 759, Oct. 19, 1996.
[2] J. A. Aardema and D. W. Koehler, "System and method for controlling an independent metering valve," U. S. Patent 5 947 140, Sep. 7, 1999.
[3] R. Book and C. E. Goering, "Programmable electrohydraulic valve," *SAE Trans.*, vol. 108, no. 2, pp. 346–352, 1999.
[4] F. Bu and B. Yao, "Adaptive robust precision motion control of single-rod hydraulic actuators with time-varing unknown inertia: A case study," in *Proc. ASME Int. Mechan. Eng. Congr. Expo.*, 1999, pp. 131–138.
[5] F. Bu and B. Yao, "Nonlinear adaptive robust control of hydraulic actuators regulated by proportional directional control valves with deadband and nonlinear flow gain coefficients," in *Proc. Amer. Control Conf.*, 2000, pp. 4129–4133.
[6] H. Du, "An E/H control design for poppet valves in hydraulic systems," in *Proc. ASME Int. Mechan. Eng. Congr. Expo.*, 2002, pp. 1–8, IMECE 2002-39350.
[7] P. M. FitzSimons and J. J. Palazzolo, "Part I: Modeling of a one-degree-of-freedom active hydraulic mount; Part II: Control," *ASME J. Dyn. Syst., Meas., Control*, vol. 118, no. 4, pp. 439–448, 1996.
[8] K. D. Garnjost, "Energy-conserving regenerative-flow valves for hydraulic servomotors," U. S. Patent 4 840 111, Jun. 20, 1989.
[9] G. C. Goodwin and D. Q. Mayne, "A parameter estimation perspective of continuous time model reference adaptive control," *Automatica*, vol. 23, no. 1, pp. 57–70, 1989.

[10] H. Hu and Q. Zhang, "Realization of programmable control using a set of individually controlled electrohydraulic valves," *Int. J. Fluid Power*, vol. 3, no. 2, pp. 29–34, 2002.
[11] H. Hu and Q. Zhang, "Multi-function realization using an integrated programmable E/H control valve," *Appl. Eng. Agriculture*, vol. 19, no. 3, pp. 283–290, 2003.
[12] A. Jansson and J.-O. Palmberg, "Seperate control of meter-in and meter-outorifices in mobile hydraulic systems," *SAE Trans.*, vol. 99, no. 2, pp. 337–383, 1990.
[13] D. N. Johnston, K. A. Edge, and N. D. Vaughan, "Experimental investigation of flow and force characteristics of hydraulic poppet and disc valves," *J. Mechan. Eng. Sci.*, vol. 205, pp. 161–171, 1991.
[14] K. D. Kramer and E. H. Fletcher, "Electrohydraulic valve system," U. S. Patent 33 846, Mar. 17, 1990.
[15] S. Liu, G. Krutz, and B. Yao, "Easy5 model of two position solenoid operated cartridge valves," in *Proc. ASME Int. Mechan. Eng. Congr. Expo.*, 2002, pp. 1–6, IMECE 2002-39335.
[16] S. Liu and B. Yao, "Energy-saving control of single-rod hydraulic cylinders with programmable valves and improved working mode selection," *SAE Trans.—J. Commercial Veh.*, pp. 51–61, 2002.
[17] H. E. Merritt, *Hydraulic Control Systems*. New York: Wiley, 1967.
[18] A. R. Plummer and N. D. Vaughan, "Robust adaptive control for hydraulic servosystems," *ASME J. Dyn. Syst., Meas., Control*, vol. 118, pp. 237–244, 1996.
[19] S. Sastry and M. Bodson, *Adaptive control: Stability, Convergence and Robustness*. Englewood Cliffs, NJ: Prentice-Hall, 1989.
[20] T. C. Tsao and M. Tomizuka, "Robust adaptive and repetitive digital control and application to hydraulic servo for noncircular machining," *ASME J. Dyn. Syst., Meas., Control*, vol. 116, pp. 24–32, 1994.
[21] T. J. Ulery, "Propotional cartridge valves—Economical alternative to large valves," *Agricultural Eng.*, vol. 71, no. 4, p. 11, 1990.
[22] N. D. Vaughan, D. N. Johnston, and K. A. Edge, "Numerical simulation of fluid flow in poppet valves," *J. Mechan. Eng. Sci.*, vol. 206, pp. 119–127, 1992.
[23] J. Watton, *Fluid Power Systems*. Englewood Cliffs, NJ: Prentice Hall, 1989.
[24] B. Yao, "High performance adaptive robust control of nonlinear systems: A general framework and new schemes," in *Proc. IEEE Conf. Dec. Control*, 1997, pp. 2489–2494.
[25] B. Yao, F. Bu, J. T. Reedy, and G. T. C. Chiu, "Adaptive robust control of single-rod hydraulic actuators: Theory and experiments," *IEEE/ASME Trans. Mechatron.*, vol. 5, no. 1, pp. 79–91, Feb. 2000.
[26] B. Yao and C. Deboer, "Energy-saving adaptive robust motion control of single-rod hydraulic cylinders with programmable valves," in *Proc. Amer. Control Conf.*, 2002, pp. 4819–4824.
[27] B. Yao and M. Tomizuka, "Smooth robust adaptive sliding mode control of robot manipulators with guaranteed transient performance," *ASME J. Dyn. Syst., Meas., Control*, vol. 118, no. 4, pp. 764–775, 1996.
[28] B. Yao and M. Tomizuka, "Adaptive robust control of SISO nonlinear systems in a semi-strict feedback form," *Automatica*, vol. 33, no. 5, pp. 893–900, 1997.
[29] B. Yao and M. Tomizuka, "Adaptive robust control of MIMO nonlinear systems in a semi-strict feedback form," *Automatica*, vol. 37, no. 9, pp. 1305–1321, 2001.

Song Liu received the Ph.D. degree from the School of Mechanical Engineering, Purdue University, Lafayette, IN, in 2005.

He is currently a Technical Supervisor and Principal Engineer with Hurco Companies, Inc., Indianapolis, IN. His research interests include advanced control theory and applications, mechatronics, multi-axis coordinated precision motion control, fluid power system control, active noise and vibration control, and dynamic stream database control.

Bin Yao (M'96) received the Ph.D. degree in mechanical engineering from the University of California, Berkeley, in 1996, the M.Eng. degree in electrical engineering from the Nanyang Technological University, Singapopre, in 1992, and the B.Eng. degree in applied mechanics from the Beijing University of Aeronautics and Astronautics, Beijing, China, in 1987.

Since 1996, he has been with the School of Mechanical Engineering, Purdue University, Lafayette, IN, and was promoted to an Associate Professor in 2002 and a Full Professor in 2007. He is one of the Kuang-piu Professors with the Zhejiang University, Zhejiang, China. His research interests include the design and control of intelligent high performance coordinated control of electromechanical/hydraulic systems, optimal adaptive and robust control, nonlinear observer design and neural networks for virtual sensing, modeling, fault detection, diagnostics, and adaptive fault-tolerant control, and data fusion. He has been actively involved in various technical professional societies such as ASME and IEEE, as reflected by the organizer/chair of numerous sessions, the member of the International Program Committee of a number of IEEE, ASME, and IFAC conferences that he has served during the past several years. He was the chair of the Adaptive and Optimal Control panel from 2000 to 2002 and the chair of the Fluid Control panel of the ASME Dynamic Systems and Control Division (DSCD) from 2001 to 2003, and currently serves as the vice-chair of the Mechatronics Technical Committee of ASME DSCD that he initiated in 2005. He was a Technical Editor of the IEEE/ASME TRANSACTIONS ON MECHATRONICS from 2001 to 2005 and currently an Associate Editor of the *ASME Journal of Dynamic Systems, Measurement, and Control*.

Dr. Yao was a recipient of the Faculty Early Career Development (CAREER) Award from the National Science Foundation (NSF) in 1998 for his work on the engineering synthesis of high performance adaptive robust controllers for mechanical systems and manufacturing processes, a Joint Research Fund for Overseas Young Scholars from the National Natural Science Foundation of China (NSFC) in 2005, and the O. Hugo Schuck Best Paper (Theory) Award from the American Automatic Control Council in 2004.